

## Amide Hydrolysis Reactivity of a N<sub>4</sub>O-Ligated Zinc Complex: Comparison of Kinetic and Thermodynamic Parameters with Those of the Corresponding Amide Methanolysis Reaction

Ewa Szajna-Fuller,<sup>†</sup> Gajendrasingh K. Ingle,<sup>†</sup> Rex W. Watkins,<sup>†</sup> Atta M. Arif,<sup>‡</sup> and Lisa M. Berreau\*<sup>†</sup>

Department of Chemistry and Biochemistry, Utah State University, Logan, Utah 84322-0300, and Department of Chemistry, University of Utah, Salt Lake City, Utah 84112

Received November 30, 2006

Treatment of the mononuclear amide-appended zinc complex [(ppbpa)Zn](ClO<sub>4</sub>)<sub>2</sub> (**1**(ClO<sub>4</sub>)<sub>2</sub>) with Me<sub>4</sub>NOH·5H<sub>2</sub>O in CD<sub>3</sub>CN/D<sub>2</sub>O (3:1) results in the formation of the deprotonated amide species [(ppbpa<sup>-</sup>)Zn]ClO<sub>4</sub> (**2**). Upon heating in CD<sub>3</sub>CN/D<sub>2</sub>O, this complex undergoes amide hydrolysis to produce a zinc carboxylate product, [(ambpa)Zn(O<sub>2</sub>CC(CH<sub>3</sub>)<sub>3</sub>)]ClO<sub>4</sub> (**3**). X-ray crystallography, <sup>1</sup>H and <sup>13</sup>C NMR, IR, and elemental analysis were used to characterize **3**. The hydrolysis reaction of **1**(ClO<sub>4</sub>)<sub>2</sub> exhibits saturation kinetic behavior with respect to the concentration of D<sub>2</sub>O. Variable-temperature kinetic studies of the amide hydrolysis reaction yielded Δ*H*<sup>‡</sup> = 18.0(5) kcal/mol and Δ*S*<sup>‡</sup> = -22(2) eu. These activation parameters are compared to those of the corresponding amide methanolysis reaction of **1**(ClO<sub>4</sub>)<sub>2</sub>.

Zinc-containing enzymes catalyze the hydrolysis of amide bonds in peptide and small molecule substrates.<sup>1</sup> Interest in elucidating mechanistic details relevant to such reactions has led to the development of synthetic model systems that exhibit amide hydrolysis reactivity.<sup>2</sup> Despite these efforts, relatively few mechanistic studies of Zn(II)-promoted amide hydrolysis reactions involving well-characterized mononuclear zinc complexes have been reported. In this regard, Groves and Chambers reported studies of an amide hydrolysis reaction involving an internal amide substrate wherein the amide carbonyl oxygen atom could not coordinate to the zinc center.<sup>3</sup> Examination of the rate of reaction as a function of temperature yielded activation parameters (Δ*H*<sup>‡</sup> = 22(1) kcal/mol and Δ*S*<sup>‡</sup> = -18(3) eu) consistent with intramolecular attack of a Zn-OH moiety on the amide carbonyl carbon in the rate-determining step.

\* To whom correspondence should be addressed. E-mail: berreau@cc.usu.edu.

<sup>†</sup> Utah State University.

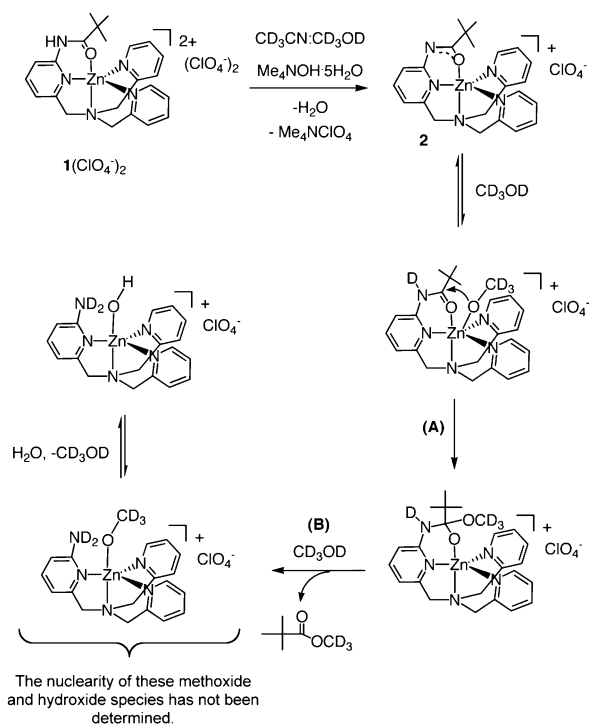
<sup>‡</sup> University of Utah.

(1) Lipscomb, W. N.; Sträter, N. *Chem. Rev.* **1996**, *96*, 2375–2434.

(2) Berreau, L. M. *Adv. Phys. Org. Chem.* **2006**, *41*, 79–181.

(3) Groves, J. T.; Chambers, R. R. *J. Am. Chem. Soc.* **1984**, *106*, 630–638.

Scheme 1

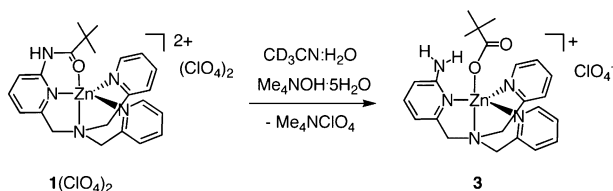


Zinc-promoted amide methanolysis reactions have been probed as analogues to the hydrolysis reactions.<sup>4</sup> We recently reported mechanistic studies of a novel zinc-promoted amide methanolysis reaction involving a zinc complex (**1**(ClO<sub>4</sub>)<sub>2</sub>, Scheme 1) with an internal amide substrate.<sup>5</sup> Activation parameters for this reaction (Δ*H*<sup>‡</sup> = 15.0(3) kcal/mol and Δ*S*<sup>‡</sup> = -33(1) eu; from an Eyring plot of second-order rate constants) are generally similar to those reported by Groves and Chambers. This led us to propose a mechanism wherein the rate-determining step of the reaction involves attack of the nucleophile at the amide carbonyl carbon ((A), Scheme

(4) Montoya-Pelaez, P. J.; Brown, R. S. *Inorg. Chem.* **2002**, *41*, 309–316.

(5) Szajna, E.; Makowska-Grzyska, M. M.; Wasden, C. C.; Arif, A. M.; Berreau, L. M. *Inorg. Chem.* **2005**, *44*, 7595–7605.

Scheme 2



1), although rate-determining breakdown of the tetrahedral intermediate cannot be ruled out (**B**), Scheme 1). A novel aspect of this proposed mechanism is the formation of a deprotonated amide intermediate (**2**) prior to the rate-determining step. Evidence for the involvement of this intermediate has been previously reported.<sup>5</sup>

To investigate how the nature of the nucleophile influences the amide cleavage reaction, we have examined the amide hydrolysis chemistry of [(ppbpa)Zn](ClO<sub>4</sub>)<sub>2</sub> (**1**(ClO<sub>4</sub>)<sub>2</sub>), ppbpa = *N*-(((6-pivaloylamido)-2-pyridyl)methyl)-*N,N*-bis((2-pyridyl)methyl)amine). Treatment of **1**(ClO<sub>4</sub>)<sub>2</sub> with Me<sub>4</sub>NOH·5H<sub>2</sub>O in acetonitrile/water (50:50) followed by heating at reflux for ~2.5 h yielded [(ambpa)Zn(O<sub>2</sub>CC(CH<sub>3</sub>)<sub>3</sub>)]ClO<sub>4</sub> (**3**; ambpa = *N*-((6-amino-2-pyridyl)methyl)-*N,N*-bis((2-pyridyl)methyl)amine)<sup>5</sup> in 71% isolated yield after workup and recrystallization (acetonitrile/water; Scheme 2). Complex **3** has been characterized by X-ray crystallography, <sup>1</sup>H and <sup>13</sup>C NMR, FTIR, and elemental analysis.

An ORTEP drawing of one of the two cations found in the asymmetric unit of **3**·0.25H<sub>2</sub>O is shown in Figure 1. The zinc center in each cation has a distorted trigonal bipyramidal geometry ( $\tau = 0.81$ , Zn(1);  $\tau = 0.94$ , Zn(2)).<sup>6</sup> In both cations the carboxylate is coordinated in a monodentate fashion.<sup>7</sup> The biggest differences between the two independent cations involve the Zn(1)–N(2)/Zn(2)–N(2A) distances (2.082(3)/2.159(3) Å), the O(1)–Zn(1)–N(2)/O(1A)–Zn(2)–N(2A) angles (104.11(11)/96.62(11)°), and bond angles of the equatorial plane.

In the <sup>1</sup>H NMR spectrum of **3** the *t*-butyl methyl resonance of the bound carboxylate is found at 1.34 ppm. This signal is upfield of the *t*-butyl methyl resonance of the amide moiety in **1**(ClO<sub>4</sub>)<sub>2</sub> (1.56 ppm) under identical conditions.

Treatment of **1**(ClO<sub>4</sub>)<sub>2</sub> with Me<sub>4</sub>NOH·5H<sub>2</sub>O in CD<sub>3</sub>CN/D<sub>2</sub>O (3:1) initially results in the formation of deprotonated amide complex [(ppbpa<sup>−</sup>)Zn]ClO<sub>4</sub> (**2**) and Me<sub>4</sub>NClO<sub>4</sub>. This zinc complex exhibits a *t*-butyl methyl resonance at 1.39 ppm.<sup>5</sup> Heating of the deprotonated amide complex in CD<sub>3</sub>CN/D<sub>2</sub>O (3:1) results in the formation of **3**. Monitoring of the disappearance of the 1.39 ppm signal of [(ppbpa<sup>−</sup>)Zn]ClO<sub>4</sub> as a function of time yielded the pseudo-first-order rate constants given in Table 1. The rate-determining step of the reaction is first-order in [(ppbpa<sup>−</sup>)Zn]ClO<sub>4</sub> (and therefore **1**(ClO<sub>4</sub>)<sub>2</sub>), as evidenced by the fact that changing the concentration of **1**(ClO<sub>4</sub>)<sub>2</sub> from 0.021 to 0.0021 M resulted in a 10-fold decrease in *k*<sub>obs</sub>.

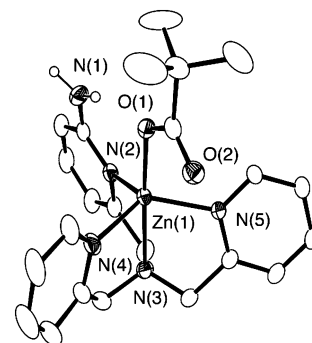


**Figure 1.** ORTEP representation of one of the two cations found in the asymmetric unit of **3**·0.25H<sub>2</sub>O. Ellipsoids are drawn at the 50% probability level. Hydrogen atoms except the amine hydrogens are not included for clarity.

**Table 1.** Observed Rate Constants for the Amide Hydrolysis Reaction of **1**(ClO<sub>4</sub>)<sub>2</sub> in CD<sub>3</sub>CN/D<sub>2</sub>O<sup>a</sup>

temp (K)	[D <sub>2</sub> O] (M)	<i>k</i> <sub>obs</sub> (s <sup>−1</sup> )
315	13.8	3.18(12) × 10 <sup>−5</sup>
325	13.8	8.37(58) × 10 <sup>−5</sup>
336	13.8	1.80(4) × 10 <sup>−4</sup>
346	13.8	4.47(23) × 10 <sup>−4</sup>
336 <sup>b</sup>	13.8	1.67(4) × 10 <sup>−4</sup>
336 <sup>b</sup>	6.90	1.49(5) × 10 <sup>−4</sup>
336 <sup>b</sup>	3.45	9.15(45) × 10 <sup>−5</sup>
336 <sup>b</sup>	1.73	5.85(35) × 10 <sup>−5</sup>
336 <sup>b</sup>	0.865	3.00(23) × 10 <sup>−5</sup>

<sup>a</sup> [1(ClO<sub>4</sub>)<sub>2</sub>] = 0.021 M in all experiments. <sup>b</sup> Reaction performed by treating **1**(ClO<sub>4</sub>)<sub>2</sub> with 1 equiv of proton sponge in CD<sub>3</sub>CN/D<sub>2</sub>O.

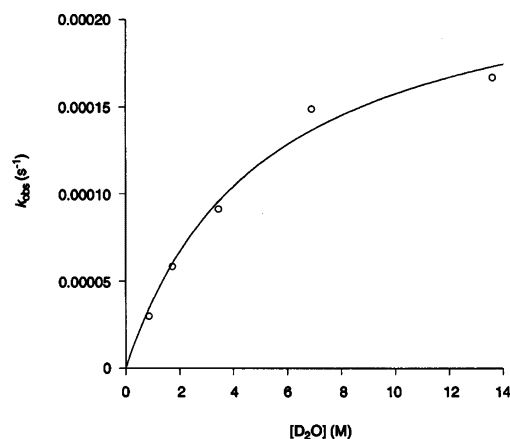


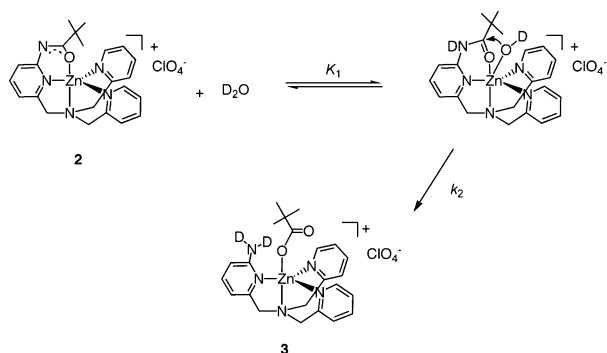
**Figure 2.** Plot of [D<sub>2</sub>O] versus *k*<sub>obs</sub> for the amide hydrolysis of **1**(ClO<sub>4</sub>)<sub>2</sub> at 336 K.

Attempts to probe the rate of the amide hydrolysis reaction of **1**(ClO<sub>4</sub>)<sub>2</sub> as a function of [D<sub>2</sub>O] initially proved problematic starting from **1**(ClO<sub>4</sub>)<sub>2</sub> and Me<sub>4</sub>NOH·5H<sub>2</sub>O in CD<sub>3</sub>CN/D<sub>2</sub>O. This may be due to the presence of waters of hydration in Me<sub>4</sub>NOH·5H<sub>2</sub>O. To avoid this problem an alternative base, proton sponge, was used. A plot of *k*<sub>obs</sub> as a function of [D<sub>2</sub>O] for the amide hydrolysis reaction is shown in Figure 2. At low concentrations of D<sub>2</sub>O, the rate of the reaction increases linearly with [D<sub>2</sub>O], consistent with a first-order dependence on the concentration of D<sub>2</sub>O in the rate-determining step. However, at higher concentrations of D<sub>2</sub>O, the rate of the reaction becomes independent of D<sub>2</sub>O concentration, indicating a mechanistic pathway that is more complicated than a single step.<sup>8</sup> This saturation behavior is consistent with a

(6) Addison, A. W.; Rao, T. N.; Reedijk, J.; van Rijn, J.; Verschoor, G. C. *J. Chem. Soc., Dalton Trans.* **1984**, 1349–1356.

(7) Kleywegt, G. J.; Wiesmeijer, W. G. R.; Van Driel, G. J.; Driessen, W. L.; Reedijk, J.; Noordijk, J. H. *J. Chem. Soc., Dalton Trans.* **1985**, 2177–2184.

Scheme 3



mechanistic pathway (Scheme 2) involving an equilibrium ( $K_1$ ) prior to an irreversible step having a rate constant  $k_2$ , as shown in eq 1. Fitting of the data to this equation yielded  $K = 0.19(4)$  and  $k_2 = 2.39(23) \times 10^{-4} \text{ s}^{-1}$ . We note that

$$k_{\text{obs}} = \frac{k_2 K_1 [\text{D}_2\text{O}]}{1 + K_1 [\text{D}_2\text{O}]} \quad (1)$$

saturation behavior in terms of methanol concentration was not found for the methanolysis reaction for concentrations of  $\text{CD}_3\text{OD}$  up to  $\sim 22 \text{ M}$  in  $\text{CD}_3\text{CN}$ .

We propose that the equilibrium in the hydrolysis reaction involves the deprotonated amide complex **2** and  $\text{D}_2\text{O}$  (Scheme 3). As we have previously described, the deprotonated amide moiety in **2** is stabilized by the presence of the Zn(II) center and via delocalization of the anionic charge into the adjacent pyridyl ring.<sup>5</sup> The proposed reactive species,  $[(d\text{-ppbpa})\text{Zn}(\text{OD})]\text{ClO}_4$ , is similar to that previously suggested for the amide methanolysis reaction. We note that analysis of the  $^1\text{H}$  NMR features of the amide hydrolysis reaction mixtures having  $[\text{D}_2\text{O}] = 13.8 \text{ M}$  did not reveal independent signals that could be assigned to the proposed reactive zinc hydroxide species. This may be due to peak overlap and/or the fact that the equilibrium ( $K_1$ ) lies toward the reactants.

An Eyring plot was constructed from variable-temperature  $k_{\text{obs}}$  values for the amide hydrolysis reaction of  $\mathbf{1}(\text{ClO}_4)_2$ . The activation parameters derived from this plot and those for the amide methanolysis reaction of  $\mathbf{1}(\text{ClO}_4)_2$ <sup>5</sup> are given

(8) Wilkins, R. G. *Kinetics and Mechanisms of Reactions of Transition Metal Complexes*, 2nd ed.; VCH Publishers: New York, 1991.

**Table 2.** Thermodynamic Data for the Amide Hydrolysis and Methanolysis Reactions of  $\mathbf{1}(\text{ClO}_4)_2$ <sup>a</sup>

	hydrolysis of $\mathbf{1}(\text{ClO}_4)_2$	methanolysis of $\mathbf{1}(\text{ClO}_4)_2$ <sup>b</sup>
$\Delta H^\ddagger$ (kcal/mol)	18.0(5)	15.0(2)
$\Delta S^\ddagger$ (eu)	-22(2)	-28(1)
$T\Delta S^\ddagger$ (kcal/mol) <sup>c</sup>	-6.6(6)	-8.3(3)
$\Delta G^\ddagger$ (kcal/mol) <sup>d</sup>	24.6(11)	23.3(5)

<sup>a</sup> Calculated using pseudo-first-order ( $k_{\text{obs}}$ ) values. <sup>b</sup> Reference 5. <sup>c</sup> 298(1) K. <sup>d</sup> Calculated from  $\Delta G^\ddagger = \Delta H^\ddagger - T\Delta S^\ddagger$  at 298(1) K.

in Table 2. These data indicate that the slower rate of amide hydrolysis of  $\mathbf{1}(\text{ClO}_4)_2$ , relative to the methanolysis reaction of the same complex (hydrolysis (315 K)  $k_{\text{obs}} = 3.18(12) \times 10^{-5} \text{ s}^{-1}$ ; methanolysis (318 K)  $k_{\text{obs}} = 2.37(12) \times 10^{-4} \text{ s}^{-1}$ ),<sup>5</sup> is due to an unfavorable increase of 3.0 kcal/mol in the enthalpy of activation ( $\Delta H^\ddagger$ ) which is offset to some degree by a smaller  $T\Delta S^\ddagger$  term. If the rate-determining step of both reactions involves, at least in part, attack of a zinc-bound nucleophile on the carbonyl carbon, the increased enthalpy of activation for the hydrolysis reaction is consistent with hydroxide ion being a poorer nucleophile than methoxide ion.

In conclusion, we have characterized the amide hydrolysis reaction of  $\mathbf{1}(\text{ClO}_4)_2$ . This reaction exhibits saturation kinetic behavior consistent with a mechanism involving equilibrium formation of a reactive species that subsequently undergoes amide hydrolysis. Comparison of the activation parameters for amide hydrolysis and methanolysis provided evidence for why the hydrolysis reaction is  $\sim 7$  times slower at  $\sim 315 \text{ K}$ . To our knowledge, this is the first direct comparison of kinetic and thermodynamic parameters of zinc-promoted amide hydrolysis and methanolysis in the same, well-characterized system.<sup>2,9</sup> These data are important, as they provide a benchmark by which to analyze zinc-promoted amide hydrolysis versus methanolysis reactions.

**Acknowledgment.** This work was supported by the National Science Foundation (CAREER Award CHE-0094066).

**Supporting Information Available:** Experimental details for the isolation and characterization of **3**; details of kinetic studies; X-ray crystallographic details (cif file) for  $\mathbf{3} \cdot 0.25\text{H}_2\text{O}$ . This material is available free of charge via the Internet at <http://pubs.acs.org>.

IC0622813

(9) Parkin, G. *Chem. Rev.* **2004**, *104*, 699–767.